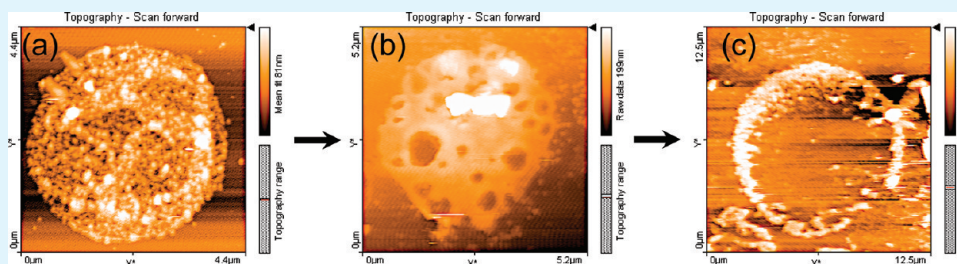


# Silver Nanoparticle Synthesis: Novel Route for Laser Triggering of Polyelectrolyte Capsules

S. Anandhakumar,<sup>†</sup> S. P. Vijayalakshmi,<sup>†</sup> G. Jagadeesh,<sup>‡</sup> and Ashok M. Raichur<sup>\*†</sup>

<sup>†</sup>Department of Materials Engineering and <sup>‡</sup>Department of Aerospace Engineering, Indian Institute of Science, Bangalore 560012, India

## ABSTRACT:



We have demonstrated the synthesis of light-sensitive polyelectrolyte capsules (PECs) by utilizing a novel polyol reduction method and investigated its applicability as photosensitive drug delivery vehicle. The nanostructured capsules were prepared via layer by layer (LbL) assembly of poly(allylamine hydrochloride) (PAH) and dextran sulfate (DS) on silica particles followed by in-situ synthesis of silver nanoparticles (NPs). Capsules without silver NPs were permeable to low molecular weight ( $M_w$ , 479 g/mol) rhodamine but impermeable to higher molecular weight fluorescence labeled dextran (FITC-dextran). However, capsules synthesized with silver NPs showed porous morphology and were permeable to higher molecular weight ( $M_w$  70 kDa) FITC-dextran also. These capsules were loaded with FITC-dextran using thermal encapsulation method by exploiting temperature induced shrinking of the capsules. During heat treatment the porous morphology of the capsules transformed into smooth pore free structure which prevents the movement of dextran into bulk during the loading process. When these loaded capsules are exposed to laser pulses, the capsule wall ruptured, resulting in the release of the loaded drug/dye. The rupture of the capsules was dependent on particle size, laser pulse energy and exposure time. The release was linear with time when pulse energy of 400  $\mu\text{J}$  was used and burst release was observed when pulse energy increased to 600  $\mu\text{J}$ .

**KEYWORDS:** silver nanoparticles, polyol reduction, polyelectrolyte capsules, laser triggering, drug delivery

## INTRODUCTION

Hollow polyelectrolyte capsules (PECs) with well-defined structures and tailorable properties have attracted considerable attention in biotechnology and promise solutions to many problems in the fields of drug delivery, biosensors, microcages and microreactors.<sup>1,2</sup> Their fabrication is based on the LbL assembly on the surface of micro- and nanoscale templates followed by dissolution of the template.<sup>3</sup> Encapsulation of macromolecules, proteins, drugs, and other bioactive materials into these PECs is of great interest due to the possibilities of using them as micro- and nanocontainers in the area of biomedical applications.<sup>2</sup> After encapsulation, the capsules can be made to release the loaded cargo in response to environmental triggers such as a change in pH, polarity, and ionic strength.<sup>4–7</sup> Such triggers have been used to tune the permeability of PECs by manipulating their intermolecular attraction in electrostatically assembled capsules. However, recent efforts have been focused on the development of other triggers such as ultrasound, magnetic, enzymatic, and laser light for remote opening of microcapsules that are unresponsive to environmental triggers.<sup>8–11</sup> Enzymes degrade the walls of the PECs to release its contents,<sup>10</sup> whereas in the case of ultrasound, the cavitation bubbles disrupt the polymer matrix.<sup>8</sup> In magnetic triggering, the application of

magnetically sensitive nanoparticles causes a drastic increase in the permeability of the capsule wall.<sup>9</sup> This permeability change is induced by the stress created due to the reorientation of nanoparticles in the magnetic field. These defined characteristics can be attributed to the PECs by either fabricating them with enzyme responsive polyelectrolytes or incorporating appropriate nanoparticles in their walls. In addition, irradiation of these capsules that contain metal NPs especially silver NPs in their walls with near infrared (NIR) radiation significantly improved the release of the encapsulated compounds.<sup>11,12</sup> Absorption of NIR radiation by Ag NPs induced heating followed by rupture of the capsule shells. In fact, the temperature increase of the suspension exposed to the beam is only about  $\sim 0.5$  K at 850 nm even with a laser of 100 mW power.<sup>13,12</sup> In addition, it is important to note that temperature increase is very localized, so any potential damage to encapsulated material is highly localized, hence there will be no loss of activity of loaded molecules. Further, the use of NIR light is particularly attractive in biomedical applications due to the weak absorption in this range by most tissues. Thus

**Received:** May 21, 2011

**Accepted:** August 23, 2011

**Published:** August 23, 2011

nanoengineering of PECs by different routes to incorporate Ag NPs in their walls should enable them to be employed for remote activated release of drugs in a controlled manner.

Generally, there are two basic methods to synthesize and stabilize silver NPs in suspension: chemical (chemical reduction, electrochemical techniques and photochemical reduction) and physical methods.<sup>14,15</sup> The most common method to prepare NPs is chemical reduction of silver ions from its salts in inorganic (sodium borohydride, hydrogen and hydrazine) or organic (citric acid, ascorbic acid, formaldehyde and reducing sugars) reducing agents. The use of strong reducing agents, for example, borohydride, resulted in nearly monodisperse small particles.<sup>16</sup> But weak reducing agents such as citrate produced larger particles at a slower reduction rate and the distribution was far from narrow.<sup>17,18</sup> So the controlled synthesis of Ag NPs was carried out in a two step reduction process: formation of smaller particles of 10–40 nm using strong reducing agents followed by particle enlargement with a weaker reducing agent to form particles of about 120–170 nm.<sup>17</sup> Furthermore, the important challenge is to extend these reaction conditions to incorporate Ag NPs in PECs, so that these capsules could be employed as drug delivery carriers and opened remotely using laser light. Previously, NPs were either deposited directly onto the capsule surface as a shell constituent or incorporated into the pre-made capsules by manipulating their permeability.<sup>11,19,20</sup> However, this often leads to inhomogeneous distribution and aggregation of NPs on the capsule surface. One solution is the in situ synthesis of Ag NPs either by performing “the silver mirror reaction” in the capsule shell before core dissolution<sup>20</sup> or reduction of AgNO<sub>3</sub> in the PSS-loaded capsules by UV/Vis irradiation.<sup>21</sup> But further studies have reported that most of the material inside the capsule was MF oligomers though it contained a small amount of PSS and Ag NPs.<sup>22</sup> Also, they were embedded as insoluble complex gel structure in the capsule, prevents capsule collapse and maintains its spherical shape even after drying. This complex can also affect the integrity of drug during encapsulation and release process. To overcome these limitations, we have introduced a single step polyol reduction process to incorporate Ag NPs of 60–120 nm directly in the walls instead of the capsule interior.<sup>23</sup> As described in our previous study, our methodology provides a means to control the size and number of NPs in the capsule shell. Such versatility will be essential in designing experiments for drug delivery.

In the present study, we demonstrate the in situ synthesis of silver NPs by polyol reduction in PAH/DS capsule walls. These capsules showed greater ability to open up polyelectrolyte capsules for laser triggered release of encapsulated substances. This is due to the fact that size, morphology, stability, and properties (chemical and physical) of metal NPs are strongly influenced by experimental conditions and the kinetics of interaction of metal ions with reducing and stabilizing agents. Variation of permeability changes of PECs prior and after silver NPs synthesis was investigated using rhodamine and FITC-dextran as probes. The precursor concentration, laser exposure time and laser intensity/energy were found to be crucial parameters influencing the release of FITC-dextran because of their direct impact on density of silver NPs incorporated in the capsule wall.

## MATERIALS AND METHODS

DS ( $M_w = 500$  kDa), PAH ( $M_w = 70$  kDa), poly(ethylene glycol) (PEG) ( $M_w = 6$  kDa), hydrofluoric acid (HF), FITC-dextran ( $M_w = 70$  kDa),

ammonium fluoride (NH<sub>4</sub>F), rhodamine (Sigma-Aldrich), and silver nitrate (Ranbaxy, India) were used without any further purification. Mono-disperse silica particles with mean diameter of  $4.27 \pm 0.25 \mu\text{m}$  were obtained from Microparticles GmbH (Germany). Milli-Q water with resistivity greater than  $18 \text{ M}\Omega \text{ cm}$  was used in this study. All pH adjustments were done with 0.1 M HCl or 0.1 M NaOH.

**Capsule Preparation.** Microcapsules were prepared by the LbL technique using silica microparticles as sacrificial templates. The silica particles (1% w/w) were alternatively coated at pH 5 by incubating them in 1 mg/mL PAH and DS polymer solution prepared with 0.2 M NaCl. After adsorption for 15 min, the microparticles were separated by centrifugation and the residual unadsorbed polyelectrolyte was removed by washing thrice with pH 5 water. After four bilayers were deposited, the silica core was dissolved in 0.1 M HF and the obtained capsules were washed and stored in water.

**Fabrication of Multilayer Capsules Incorporated with Silver NPs.** The preparation and deposition of silver NPs have been reported earlier.<sup>19</sup> This involved the sequential adsorption of three layers of PAH and DS on silica microparticles followed by silver NPs synthesis. AgNO<sub>3</sub> was used as precursor for the formation of silver NPs and reduction was performed at 50° C in the presence of PEG. After synthesis of silver NPs, the coated particles were washed and deposited with another bilayer of PAH and DS. Then the silica core was dissolved with HF buffer (0.1 M HF:0.5 M NH<sub>4</sub>F) to yield silver NPs incorporated hollow capsules. Two different sizes of silver NPs were deposited in the PECs by changing the AgNO<sub>3</sub> concentration from 25 to 50 mM.<sup>23</sup> Then the capsules were washed three times with water and used for laser illumination experiments.

**Encapsulation of FITC-Dextran.** FITC-dextran was encapsulated inside the polyelectrolyte capsules by thermal encapsulation method. The silver NPs synthesized capsule suspension was mixed with FITC-dextran for 1 h and incubated at 70° C for 1 h. Polyelectrolyte capsules without silver NPs filled with FITC-dextran and used as control capsules. For control capsules, the encapsulation was carried out by mixing capsule suspension with FITC-dextran at pH 3.5 in 0.2 M NaCl solution for 1 h and incubated at 70° C for 1 h as mentioned previously.

**Laser Irradiation Study.** The laser experiments involved irradiating the capsule suspensions (with and without light absorbing silver NPs) in a 3 ml quartz cuvette to investigate their rupture behavior on exposure to laser light. Irradiation was performed with a laser beam of 530 nm, 10 Hz series of 7 ns pulses from neodymium:yttrium–aluminum–garnet (Nd:YAG) laser (Quanta-Ray, Spectra-Physics, USA). The influence of parameters such as NP size, exposure time and laser intensity on rupture was investigated to estimate the time of rupture. This enables us to modulate the release profile during release studies. After irradiation, the capsules were analyzed in transmission electron microscopy (TEM)/ atomic force microscopy (AFM) to visualize the morphological changes occurred on the capsule surface.

For release studies, the capsules loaded with FITC-dextran were exposed to laser pulse of 400  $\mu\text{J}$  for various time intervals in order to find out the possibility to modify the release profile. After exposure, the capsules were centrifuged and fluorescence spectra for FITC-dextran in the supernatants obtained were recorded at 490 nm (excitation wave length of FITC-dextran).

**Characterization.** Confocal images of polyelectrolyte capsules in water were observed using a Zeiss LSM 510 META confocal scanning system (Zeiss, Germany) equipped with a 100x/1.4–1.7 oil immersion objective. To visualize the capsules, molecular probes of different sizes and charges such as rhodamine and FITC-dextran were used. During CLSM imaging, the other parameters such as aperture, gain and laser power were kept constant to avoid over saturation of fluorescence signal. Fluorescence spectra of the released dextran were recorded using a Jobin Yvon Fluorolog3 spectrofluorimeter (Horiba Scientific Instruments, USA). For AFM analysis, a drop of capsule suspension was placed on

a silicon wafer and air dried overnight. Then the samples were characterized using a Nanosurf Easy Scan2 AFM (Nanoscience Instruments Inc, USA) in air at room temperature by contact mode. FE-TEM measurements were performed on a Tecnai F30 (FEI, Eindhoven, Netherlands) microscope operating at 200 kV.

## RESULTS AND DISCUSSION

Polyol chemistry in combination with LbL assembly of polyelectrolytes was used to synthesize silver NPs in polyelectrolyte capsules. Typical AFM images of the capsules before and after synthesis of silver nanoparticles are shown in Figure 1a,b. Figure 1a shows the morphology of pure polyelectrolyte capsule (without silver NPs) which exhibits folds and creases that are typical of hollow capsules. After synthesis of silver NPs, the capsule showed thicker shell than the original polyelectrolyte capsule due to the formation of silver NPs within the shell. It can be seen that the capsules were rough and had a mesh kind of surface morphology when incorporated with spherical silver nanoparticles (Figure 1b). The formation of silver NPs prevents the formation of folding and creases unlike pure polyelectrolyte capsules. In order to investigate the inner structure of NPs loaded capsules, they were analyzed by TEM. Figure 1c shows that the silver NPs are homogeneously distributed and mostly occurs inside the capsule shell. On the basis of AFM and TEM measurements, the size of silver NPs produced was found to be  $60 \pm 20$  nm, which can be further modulated by varying the concentration of  $\text{AgNO}_3$ .<sup>23</sup>

In perspective of using these capsules as drug delivery vehicles for remote-activated release, we investigated the permeability of the capsules prior and after nanoparticle formation to fluorescent probes of different sizes. We used rhodamine as well as FITC-dextran as models of biologically active molecules of various hydrodynamic radius to study the wall permeability using CLSM. Confocal images of pure polyelectrolyte capsules in rhodamine and FITC-dextran (70 kDa) showed that the former is permeable whereas latter is impermeable even after one hour of incubation in the probe solution as shown in Figure 2a,b. This size exclusion is attributed to the size of the pores that are present on the capsule surface, because the permeability of the probe molecules depends on molecular size cut off of the capsule wall, which in turn is fixed by these surface pores. The apparent mesh size of the capsule wall can be estimated from the hydrodynamic radius of rhodamine and dextran, since it is permeable for rhodamine and impermeable for FITC-dextran (hydrodynamic diameter is 0.6 nm for rhodamine and 6.6 nm for FITC-dextran).<sup>24</sup> Therefore, the capsules have an apparent mesh size of  $\leq 6$  nm which makes them permeable to only low molecular weight probe molecules like rhodamine. A similar size exclusive behavior has been reported for chitosan/chitosan sulfate capsules at pH 6 which were impermeable to FITC-dextran with  $M_w$  above  $2 \times 10^5$  Da.<sup>25</sup> On the other hand, the silver NPs incorporated capsules are permeable to both probe molecules as shown in Figure 2c&d. The nanoparticle formation during the synthesis resulted in significant increase in mesh size of the capsule shell. The fluorescence signal was observed from the capsules interior as well as bulk which confirmed the presence of larger pores of diameter greater than 6.6 nm in the capsule shell. Similar observation of increased permeability towards high molecular weight dextran ( $M_w = 2 \times 10^6$  Da) was reported when ferromagnetic gold/cobalt nanoparticles were embedded into the capsule shell.<sup>26</sup> This mesh size increment can be attributed to

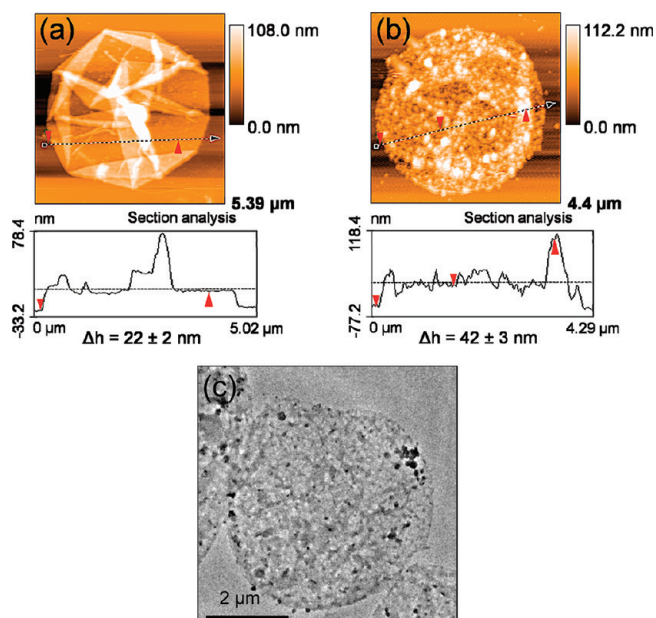


**Figure 1.** Morphology analysis to show the deposition of silver nanoparticles in the PAH/DS capsule shell at 25 mM  $\text{AgNO}_3$  concentration. AFM images of hollow capsules (a) without and (b) with incorporated silver NP and (c) corresponding TEM image of silver NP incorporated capsules.

the pores within the multilayers, probably defects and discontinuities caused by silver nanoparticles. After synthesis of silver NPs, pores of several nanometers to tens of nanometers in diameter and  $20 \pm 5$  nm in depth on the capsule surface were observed together with increase of roughness from  $6 \pm 2$  nm (for pure polyelectrolyte capsules) to  $13 \pm 2$  nm (NPs deposited capsules) over an area of  $500 \text{ nm} \times 500 \text{ nm}$  in AFM investigation (Figure 1a,b). It is important to note that the walls of silver NPs deposited capsules appeared darker when compared to pure polyelectrolyte capsules, which is due to the presence of silver NPs in the capsules wall.

Because of the porous nature of silver NP incorporated capsules, thermal encapsulation method was used for encapsulation among other most widely used methods such as changing the pH, solvent and ionic strength. This method involves the heat treatment of capsules suspension in the presence of low molecular weight compounds, exploiting the decrease in permeability for encapsulation.<sup>27</sup> In this work, FITC-dextran of 70 kDa was employed as the probe macromolecule because it penetrates the silver loaded capsules but not the pure polyelectrolyte capsules. Figure 3 shows the confocal images of capsules with and without silver NPs incubated in FITC-dextran at  $70^\circ \text{C}$  for 30 min. It can be seen that both the capsules maintain their spherical shape but shrink significantly on heat treatment. As pure polyelectrolyte capsules are impermeable to dextran, heat treatment makes them further difficult to permeate dextran and appears darker (Figure 3a). But, in the case of silver NP deposited capsules, the shell shrinkage and densification induced by heat treatment prevents the movement of permeated dextran from the capsule interior into bulk and hence enrichment occurs inside the capsules. From the observation of fluorescent signal, it can be concluded that the Ag NP incorporated capsules showed good loading of FITC-dextran inside the capsules (Figure 3b), whereas pure polyelectrolyte capsules hardly showed any loading due to

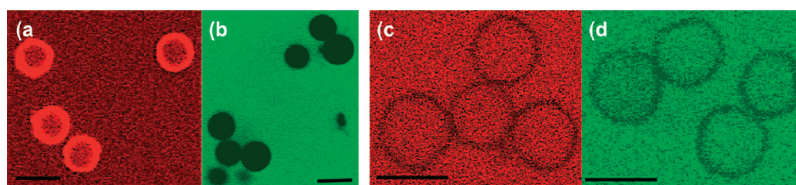


**Figure 2.** CLSM images to show open and closed state of control (without NPs) and silver NPs incorporated capsules. (a, b) Control capsules and (c, d) silver NPs incorporated capsules treated with rhodamine (a, c) and FITC-dextran of 70 kDa (c, d). Scale bar = 5  $\mu\text{m}$ .

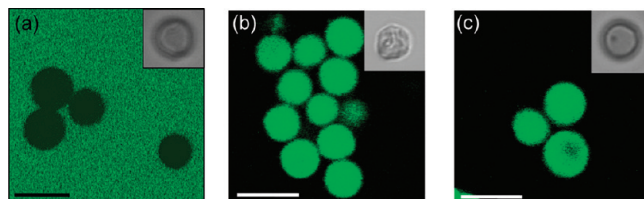


**Figure 3.** CLSM images to show the encapsulation of 70 kDa dextran (green fluorescence) after heat treatment for 1 h. (a) Control capsules, (b) silver NPs incorporated capsules and (c) control capsules at pH 3 in the presence of 0.2 M NaCl. Insets shows transmission images of the respective control and silver NPs incorporated capsules. The capsule surface appears smooth in control capsules which transforms into rough folded structure after synthesizing silver NPs. Scale bar = 5  $\mu\text{m}$ .

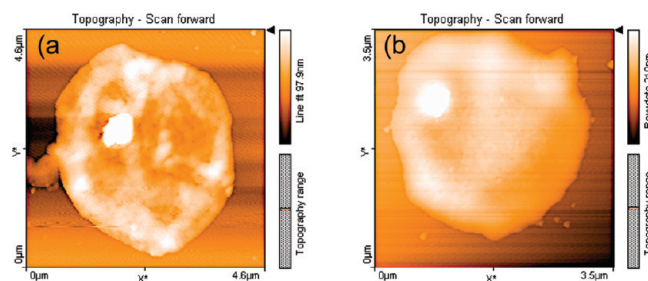


**Figure 4.** AFM analysis of silver NPs incorporated capsules under heat treatment at different time intervals: (a) 0.5 and (b) 1 h.

their impermeable nature prior to and after heat treatment (Figure 3a). For control experiments, the pure polyelectrolyte capsules were loaded with dextran at pH 3.5 in 0.2 M NaCl by heat treatment process exploiting the pH dependent wall permeability as shown in Figure 3c. The insets in the CLSM images show the transmission images of the corresponding capsules in suspension. The loaded capsules appeared swollen and bulky when compared to unloaded ones because of the encapsulation of dextran. Further, it can be seen that the silver NP deposited capsules showed swollen structure with partially folded shell because the presence of silver NPs prevents the swelling of the capsules when compared to that of control capsules.

To investigate the morphological changes of silver NP deposited capsules under heat treatment, we analyzed them by AFM at different time intervals. AFM images of dried capsules incubated in pure water at 70° C for various time intervals are shown in Figure 4. The silver NP incorporated capsules after heat treatment tend to collapse partially on drying and form a flat structure without pores and defects on the surface. It is known that heat treatment heals the defects and pores within the multilayers and smoothens the surface. This could be further supported by roughness analysis where surface roughness

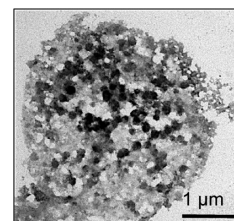


**Figure 5.** TEM investigation to show the rupture of silver NPs deposited capsule after exposing to laser pulses for 5 s at pulse energy of 400  $\mu\text{J}$ .

reduced from  $13 \pm 2$  nm to  $7 \pm 2$  nm after heat treatment for 1 h over an area of 500 nm  $\times$  500 nm. These capsules did not maintain the spherical shape in the dried form unlike the pure polyelectrolyte ones under heat treatment,<sup>28</sup> possibly because of the presence of large number of silver NPs within the shell to destabilize or collapse the spherical shape. Thus these results indicate that the porous morphology formed during the NPs synthesis can be effectively utilized for encapsulation of FITC-dextran without any additional changes in pH, salt and polarity etc., to open up the capsules at the time of encapsulation.

The influence of laser irradiation on the permeability and release of the encapsulated FITC-dextran from the capsules was investigated since these capsules can have potential advantage in remote-activated release of drug/biomolecules in biomedical applications. For laser irradiation studies, laser of 530 nm was chosen which is located close to the surface plasmon resonance absorption band of silver NPs ( $\sim 450$  nm). The laser illumination of control and silver NPs deposited capsules showed different results under same illumination conditions. Polyelectrolyte capsules with silver NPs were ruptured and deformed after illumination while no such changes were observed in pure polyelectrolyte capsules. Figure 5 shows the TEM image of the ruptured capsules after laser illumination. The silver NPs deposited capsules showed that discrete shell of individual capsules were no longer visible and appeared like patchy, rough and discontinuous surface. The deposited silver NPs can be seen clearly over the surface of the ruptured capsules. However, hardly any changes were observed in control capsules (image not shown). The silver NPs present in the polyelectrolyte shell act as energy absorption centers, heat up the capsule shell and induces rupture during laser irradiation.<sup>19</sup> These results confirmed that NPs incorporated by novel polyol reduction method can be efficiently used to induce the release of dextran when exposed to NIR radiation.

The rupture of the capsule was found to be dependent on many parameters, i.e., the size, distribution and number of silver NPs incorporated in the shell, the intensity of laser and exposure time used for illumination. We have investigated how significant these parameters are in the rupturing of the capsules and

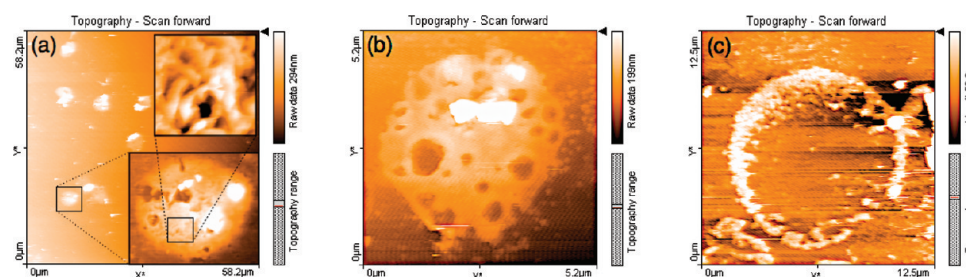


**Figure 6.** AFM investigations to show rupturing of silver NPs deposited capsules under laser exposure. Ruptured capsules after (a) 5, (b) 8, and (c) 10 s of laser exposure. Insets show the zoomed cross-section areas of the image marked in rectangular boxes.

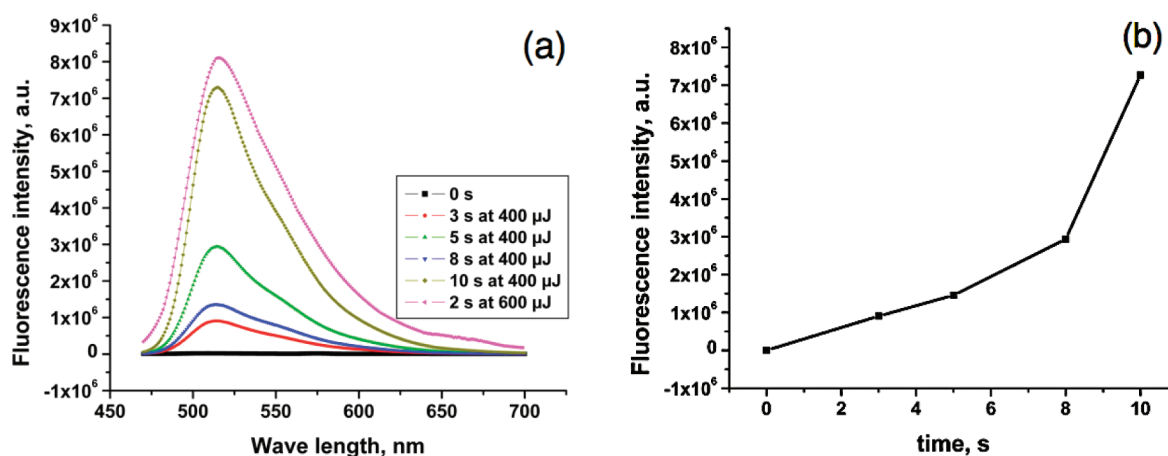


**Figure 7.** (a) Fluorescence spectra of released FITC-dextran as a function of exposure time and pulse energy and (b) fluorescence intensity of released dextran at 515 nm with exposure time.

consequently the release of dextran. Two different types of capsules containing  $60 \pm 20$  nm and  $100 \pm 20$  nm size silver NPs were prepared and used to investigate the size effect on capsule rupture under laser treatment. First, both capsules were irradiated by laser pulse of  $400 \mu\text{J}$ , which led to the rupture and release of dextran regardless of the capsule type. However, their rupture or deformation time varies distinctly as a function of size of silver NPs present in the capsules. The time required to rupture the capsule shell was 5 s, which decreased to 2–3 s when the nanoparticle size increased from  $60 \pm 20$  nm to  $100 \pm 20$  nm. This is due to the fact that metal NPs of larger sizes are heated faster than the smaller ones hence enhance absorption and local heating. Therefore, the capsules containing larger NPs get ruptured faster than the ones with smaller NPs.<sup>11</sup> It is also important to note that the degree and speed of rupture depends on interaction of silver NPs between themselves as well as their distribution within the shell. The number of silver NPs present in the capsules that contain  $100 \pm 20$  nm particles were higher and also distributed randomly throughout the capsule shell. Therefore, it can be concluded that the random distribution of larger particles caused faster heating than smaller particles of uniform distribution and thus induced faster rupture in the capsule shell.

In the second case, capsules containing  $100 \pm 20$  nm size particles were illuminated with a laser pulse of  $400 \mu\text{J}$  and their morphological changes were studied by varying the exposure time. AFM was used to investigate the influence of exposure time on morphological changes due to rupture. It shows that the rupture starts at 5 s where the morphology transforms into wavy structure with newly formed nanopores of size around 50–100 nm

(Figure 6a). It is interesting to note that all the capsules were ruptured uniformly. When the exposure time was increased, the nanopores merge and grow into larger size ranging from 200–500 nm as shown in Figure 6b. However, complete rupture of capsules into tiny pieces was observed when the exposure time reached 10 s and there was evidence of silver NPs among the remnants of the capsules (Figure 6c). Finally, the speed and degree of rupture further depends on the energy of laser used for irradiation. At lower laser energy of  $400 \mu\text{J}$ , the rupturing time was around 5 s, but it reduced into <2 s when the energy increased to  $600 \mu\text{J}$ . Because the rupture occurred instantaneously, it was difficult to estimate the exact rupturing time once the capsules suspension was exposed to the laser beam. These results indicate that by choosing appropriate NPs size, exposure time, and laser intensity, one can modulate their absorption properties and thus control the rupture of the capsules.

To investigate the release of dextran, the dextran loaded capsules (both the control as well as silver NPs deposited capsules) were illuminated with a laser pulse of  $400 \mu\text{J}$  for various time intervals. After illumination, the capsule suspension was centrifuged and FITC-dextran fluorescence emission from the supernatant was recorded. The fluorescence signal of high intensity at 515 nm corresponding to FITC-dextran was observed for the silver NPs incorporated capsules. The fluorescence intensity increased with exposure time initially and reached a saturation value as shown in the Figure 7a. The intensity at 515 nm was plotted against time, which shows that the release is almost linear up to 8 s (Figure 7b) and increases suddenly once the capsules started to break into fragments as shown previously

in Figure 6c. However exposing these capsules to a laser pulse of 600  $\mu$ J, fluorescence intensity at 515 nm directly shoots up to the maximum value and there was no further change. It shows that the release of dextran can be varied from linear (controlled) to burst release by modifying the exposure time and laser intensity. On the contrary, no such fluorescence signal was observed from the samples without silver NPs in their capsule shell. This shows that the silver NPs synthesized by polyol route effectively induced the release of FITC-dextran from the capsules when exposed to NIR radiation whereas capsules without silver NPs remain unaffected by laser radiation. These results confirmed that such capsules can be used as light responsive vehicles in the area of drug delivery applications.

## CONCLUSION

We have demonstrated a novel approach to incorporate silver NPs in the PECs shell for photoinduced release of encapsulated substances for biological applications. After silver NPs were synthesized, the capsules were permeable to FITC-dextran of 70 kDa because of pores created by the presence of NPs. The capsules containing larger NPs get ruptured faster than the capsules that contain smaller silver NPs. The rupture of the capsules is significantly influenced by the parameters such as NP size and their distribution, laser energy, and time of exposure. The release studies shown that the silver NPs deposited by this method could be efficiently used to induce release of FITC-dextran when exposed to laser beam. The release rate could be varied from linear to burst release. The rate of release is a function of time and applied pulse energy. It is important to note that the green approach demonstrated here shows great promise in the area of biomedical and biotechnology, particularly drug delivery, as it is a versatile method to tailor the release in a controlled manner.

## AUTHOR INFORMATION

### Corresponding Author

\*Phone: +91-80-22933238. Fax: +91-80-23600472. E-mail: amr@materials.iisc.ernet.in.

## ACKNOWLEDGMENT

The authors thank the Institute Nanoscience Initiative, Indian Institute of Science for microscopy facility and Prof. S. Ramakrishnan, Department of Inorganic and Physical Chemistry for fluorescence spectrometer. This work is supported by Dow Chemical International Pvt. Ltd., India.

## REFERENCES

- (1) De Geest, B. G.; Vandenbroucke, R. E.; Guenther, A. M.; Sukhorukov, G. B.; Hennink, W. E.; Sanders, N. N.; Demeester, J.; De Smedt, S. C. *Adv. Mater.* **2006**, *18*, 1005.
- (2) Peyratout, C. S.; Dähne, L. *Angew. Chem., Int. Ed.* **2004**, *43*, 3762.
- (3) Donath, E.; Sukhorukov, G. B.; Caruso, F.; Davis, S. A.; Möhwald, H. *Angew. Chem., Int. Ed.* **1998**, *37* (16), 2201.
- (4) Anandhakumar, S.; Nagaraja, V.; Raichur, A.M. *Colloids Surf., B* **2010**, *78*, 266.
- (5) Sukhorukov, G.B.; Antipov, A.A.; Voigt, A.; Donath, E.; Möhwald, H. *Macromol. Rapid Commun.* **2001**, *22*, 44.
- (6) Lvov, Y.; Antipov, A.A.; Mamedov, A.; Möhwald, H.; Sukhorukov, G.B. *Nano Lett.* **2001**, *1* (3), 125.

- (7) Ibarz, G.; Dähne, L.; Donath, E.; Möhwald, H. *Adv. Mater.* **2001**, *13* (17), 1324.
- (8) Shchukin, D.G.; Gorin, D.A.; Möhwald, H. *Langmuir* **2006**, *22*, 7400.
- (9) Lu, Z.; Prouty, M. D.; Guo, Z.; Golub, V.O.; Kumar, C. S. S. R.; Lvov, Y. M. *Langmuir* **2005**, *21*, 2042.
- (10) Itoh, Y.; Matsusaki, M.; Kida, T.; Akashi, M. *Biomacromolecules* **2006**, *7*, 2715.
- (11) Radziuk, D.; Shchukin, D.G.; Skirtach, A.; Möhwald, H.; Sukhorukov, G. *Langmuir* **2007**, *23*, 4612.
- (12) Skirtach, A.G.; Antipov, A.A.; Shchukin, D.G.; Sukhorukov, G. B. *Langmuir* **2004**, *20*, 6988.
- (13) Schönle, A.; Hell, S. W. *Opt. Lett.* **1998**, *23*, 325.
- (14) Chen, W.; Cai, W.; Zhang, L.; Wang, G.; Zhang, L. *J. Colloid Interface Sci.* **2001**, *238*, 291.
- (15) Frattini, A.; Pellegrini, N.; Nicastro, D.; De Sanctis, O. *Mater. Chem. Phys.* **2005**, *94*, 148.
- (16) Creighton, J.; Blatchford, C.; Albrecht, M. *Photochem. Photobiol.* **1994**, *60*, 605.
- (17) Lee, P. C.; Meisel, D. *J. Phys. Chem.* **1982**, *86*, 3391.
- (18) Shirtcliffe, N.; Nickel, U.; Schneider, S. *J. Colloid Interface Sci.* **1999**, *211*, 122.
- (19) Angelatos, A. S.; Radt, B.; Caruso, F. *J. Phys. Chem. B* **2005**, *109*, 3071.
- (20) Parakhonskiy, B.V.; Bedard, M.F.; Bukreeva, T.V.; Sukhorukov, G.B.; Möhwald, H.; Skirtach, A.G. *J. Phys. Chem. C* **2010**, *114*, 1996.
- (21) Shchukin, D. G.; Radtchenko, I. L.; Sukhorukov, G. B. *Chemphyschem* **2003**, *4*, 1101.
- (22) Sukhorukov, G. B.; Shchukin, D. G.; Dong, W. F.; Möhwald, H.; Lulevich, V. V.; Vinogradova, O. I. *Macromol. Chem. Phys.* **2004**, *205*, 530.
- (23) Anandhakumar, S.; Raichur, A.M. *Colloids Surf., B* **2011**, *84*, 379.
- (24) Andrieux, K.; Lesieur, P.; Lesieur, S.; Ollivon, M.; Grabielle-Madlmont, C. *Anal. Chem.* **2002**, *74*, 5217.
- (25) Berth, G.; Voigt, A.; Dautzenberg, H.; Donath, E.; Möhwald, H. *Biomacromolecules* **2002**, *3*, 579.
- (26) Lu, Z.H.; Prouty, M. D.; Guo, Z.H.; Golub, V.O.; Kumar, C.; Lvov, Y. M. *Langmuir* **2005**, *21*, 2042.
- (27) Köhler, K.; Sukhorukov, G.B. *Adv. Funct. Mater.* **2007**, *17*, 2053.
- (28) Köhler, K.; Shchukin, D.G.; Sukhorukov, G.B.; Möhwald, H. *Macromolecules* **2004**, *37*, 9546.